GEOPHYSICAL RESEARCH LETTERS, VOL. 36, L07708, doi:10.1029/2008GL036874, 2009



# The pacemaker of major climate shifts

Geli Wang,[1] Kyle L. Swanson,[2] and Anastasios A. Tsonis[2]

Received 2 December 2008; revised 21 January 2009; accepted 3 February 2009; published 15 April 2009.

[1] Models and data suggest that the interplay of major climate modes may result in climate shifts. More specifically it has been shown that when the network of North Atlantic Oscillation (NAO), Pacific Decadal Oscillation (PDO), El Nino/Southern Oscillation (ENSO) and North Pacific Index (NPI) synchronizes, an increase in the coupling between these oscillations destroys the synchronous state and leads the climate system to a new state. These shifts are associated with significant changes in global temperature trend and in ENSO variability. Here we probe the details of this network's dynamics to investigate if a certain oscillation is the culprit in these shifts. From a total of 12 synchronization events observed in three climate simulations and in observations we find that the instigator of these shifts is NAO. Without exception only when NAO's coupling with the Pacific increases a shift will occur. Our results suggest a dynamical sequence of events in the evolution of climate shifts which is consistent with recent independent empirical and modeling studies. **Citation:** Wang, G., K. L. Swanson, and A. A. Tsonis (2009), The pacemaker of major climate shifts, *Geophys. Res. Lett.*, *36*, L07708, doi:10.1029/2008GL036874.

## 1. Introduction and Previous Results

[2] An important aspect of the theory of synchronization between coupled nonlinear oscillators is coupling strength. The theory of synchronized chaos [*Pecora et al.*, 1997; *Boccaletti et al.*, 2002] predicts that in many cases when such systems synchronize, an increase in coupling strength between the oscillators may destroy the synchronous state and alter the system's behavior. These ideas have lately been explored in a network of four climate oscillators, namely ENSO, NAO, NPI, and PDO [*Tsonis et al.*, 2007]. These modes represent regional but dominant modes of climate variability in the northern hemisphere, with time scales ranging from months to decades. These modes may be correlated to some degree as the action of one may trigger the action of another. However, each of these modes involves different mechanisms over different geographical regions. NAO [*Hurrell*, 1995] and NPI [*Trenberth and Hurrell*, 1994] are the leading modes of surface pressure variability in northern Atlantic and Pacific Oceans, respectively, the PDO [*Mantua et al.*, 1997] is the leading mode of SST variability in the northern Pacific and ENSO [*Philander*, 1990] is a major signal in the tropical Pacific. Together these four modes capture the essence of climate variability in the northern hemisphere.

[3] In an earlier work [*Tsonis et al.*, 2007] we showed that this network may indeed synchronize. Consistent with the theory of synchronized chaos we also showed that when a synchronization event is followed by an increase in the overall coupling strength, then the synchronous state is destroyed and after that climate emerges in a different state, which is characterized by significant changes in global temperature trend and in ENSO variability. Those results were based on 10 synchronization events observed in two climate model simulations. The model was the GFDL CM2.1 coupled ocean/atmosphere model. The first simulation is an 1860 pre-industrial conditions control run and the second is the SRESA1B, which is a "business as usual" scenario with $CO_2$ levels stabilizing at 720 ppmv at the close of the 21st century. Synchronization is measured by the distance of the network and the coupling strength by how well the phases of the four mode indices can be predicted [*Tsonis et al.*, 2007; *Smirnov and Bezruchko*, 2003] (see auxiliary material for more details).[1] Figure 1a shows one of those events. The broken line shows the distance of the network as a function of time estimated over a sliding window of 11 years. The horizontal dotted line is the 95% confidence level associated with the null hypothesis that the observed mode indices are sampled from a population of a correlated multi (four) AR-1 process where the correlations are the lag zero cross-correlations between all pairs of the observed modes. According to this graph, the network shows statistically significant synchronization in the period 1932-1943. The solid line shows the coupling strength as a function of time. Note that according to the definition of coupling, higher values correspond to weaker strength. We observe that during the early stages of this synchronization event the coupling strength decreases. In this early period no changes in global temperature trend or in ENSO variability are documented. The coupling strength begins to increase around 1939 and it keeps on increasing until the network goes out of synchronization around 1942-43. The destruction of this state coincides with a well known climate shift characterized by a sharp change in global temperature trend (see Figure 1b) and by a change from more frequent and strong El Ninos to more frequent and strong La Ninas (Figure 1c). This behavior was observed without exception in all synchronization events reported by *Tsonis et al.* [2007], when synchronization was followed by an increase in coupling strength. Since the publication of these results we have confirmed this behavior in two more synchronization events observed in an additional simulation this time from the ECHAM5 climate model, and the statistical significance of the shifts has been assessed (see auxiliary material). The mechanism of synchronization followed by an increase in coupling leading

[1] Institute of Atmospheric Physics, Chinese Academy of Sciences, Beijing, China.
[2] Atmospheric Sciences Group, Department of Mathematical Sciences, University of Wisconsin-Milwaukee, Milwaukee, Wisconsin, USA.


0094-8276/09/2008GL036874$05.00

[1] Auxiliary materials are available in the HTML. doi:10.1029/2008GL036874.

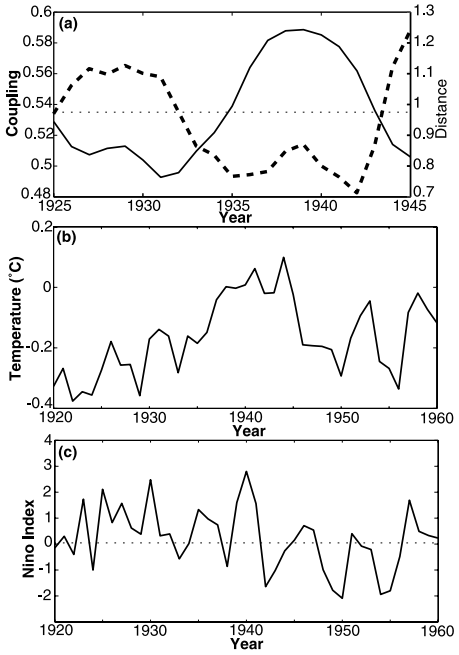


**Figure 1.** (a) The broken line shows the distance of a network consisting of four observed major climate modes as a function of time in the period 1925–1945. This distance is an indication of synchronization between the modes with smaller distance implying stronger synchronization. The parallel dotted line represents the 95% significance level associated with a null hypothesis of spatially correlated red noise. Accordingly the network is synchronized from 1932 to 1943. The solid line shows the coupling strength between the four modes as a function of time (for the definition of distance and coupling strength see ref. 15 or auxiliary material). (b) The CRU global temperature record in the period 1920 to 1960. Note the sharp change in trend around 1943 [from *Brohan et al.*, 2006]. (c) Nino Index in the period 1920 to 1960. Note the sharp change from frequent El Ninos to frequent La Ninas.

to a change in climate behavior seems to be rather robust. For example, it remains in a larger network that includes other oceanic and atmospheric flow indices (such as the Atlantic Multidecadal Oscillation (AMO) [*Kerr*, 2000], the Western Pacific pattern (WP) [*Wallace and Gutzler*, 1981; *Barnston and Livezey*, 1987], the Tropical North Atlantic index (TNA) [*Enfield et al.*, 1999], and the Pacific North America Pattern (PNA) [*Barnston and Livezey*, 1987], albeit the signal is stronger when only the four indices are used. This is possibly because inclusion of more (secondary) modes may mask the interplay of the major modes. Thus, larger networks may not offer additional information in this particular approach.

## 2. New Analysis and Results

[4] Our results given by *Tsonis et al.* [2007] refer to the collective behavior of the four major modes used in the network. As such they do not offer insights on the specific details of the mechanism. For example, do small distance values (strong synchronization) result from all modes synchronizing or from a subset of them? When the network is

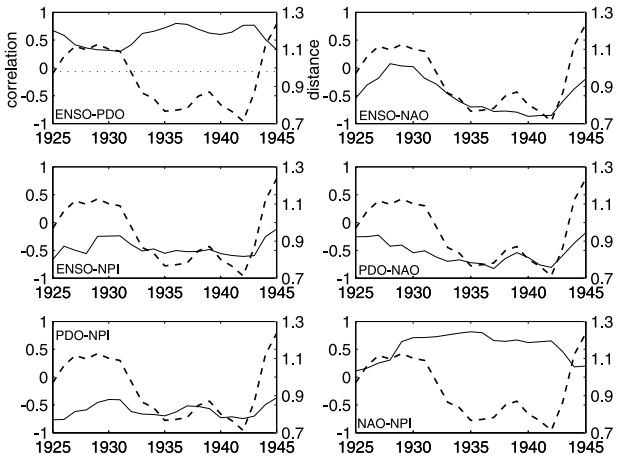


**Figure 2.** The broken line in all panels is the distance of the complete network of the four modes. The parallel dotted line represents the 95% significance level associated with a null hypothesis of spatially correlated red noise (same as in Figure 1). The solid line on each plot indicates the correlation coefficient between all possible six pairs as function of time (estimated over a sliding window of 11 years). See text for details.

synchronized, does the coupling increase require that all modes must become coupled with each other? To answer these questions we split the network of four modes into its six pair components and we investigate the contribution of each pair in each synchronization event and in the overall coupling of the network. Figures 2 and 3 illustrate in detail our approach by focusing in the synchronization event described in Figure 1. The broken line in all panels is the distance of the complete network of the four modes (same as in Figure 1). The solid line on each plot in Figure 2 indicates the correlation coefficient between all possible six pairs as function of time (estimated over a sliding window

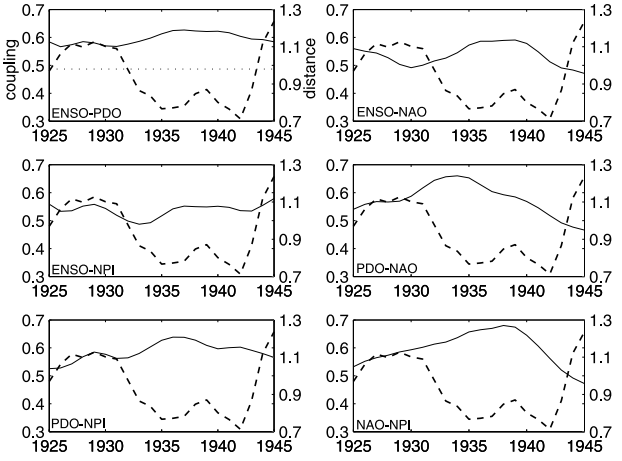


**Figure 3.** The broken line in all panels is the distance of the complete network of the four modes. The parallel dotted line represents the 95% significance level associated with a null hypothesis of spatially correlated red noise (same as in Figure 1). The black line on each plot shows the coupling strength between all possible six pairs as function of time. See text for details.

**Table 1.** Synchronized Events of Model Simulations and Observations[a]

| Synchronization Event | Occurring in | Synchronized Pairs | Coupling Strength Increases Between | Climate Shift? |
|---|---|---|---|---|
| 1 | Observations 1910–1913 | ENSO-PDO<br>ENSO-NPI<br>PDO-NAO | ENSO-PDO<br>ENSO-NPI<br>PDO-**NAO**<br>PDO-NPI<br>**NAO**-NPI | YES |
| 2 | Observations 1921–1925 | ENSO-NPI<br>PDO-NPI | None of the pairs | NO |
| 3 | Observations 1932–1939 | ENSO-PDO<br>ENSO-NAO<br>PDO-NPI<br>PDO-NAO<br>NAO-NPI | None of the pairs[b] | NO |
| | Observations 1939–1943 | ENSO-PDO<br>ENSO-NAO<br>PDO-NPI<br>PDO-NAO<br>NAO-NPI | ENSO-**NAO**<br>PDO-**NAO**<br>**NAO**-NPI | YES |
| 4 | Observations 1952–1957 | ENSO-PDO<br>ENSO-NPI<br>PDO-NPI | ENSO-PDO<br>PDO-NPI | NO |
| 5 | Observations 1975–1979 | ENSO-NAO<br>PDO-NPI | ENSO-PDO<br>ENSO-NPI<br>PDO-**NAO**<br>PDO-NPI | YES |
| 6 | GFDL CM2.1 Control run Years 120–129 | ENSO-PDO<br>ENSO-NPI<br>ENSO-NAO<br>PDO-NAO<br>PDO-NPI<br>NAO-NPI | PDO-**NAO**<br>PDO-NPI<br>**NAO**-NPI | YES |
| 7 | GFDL CM2.1 Control run Years 140–148 | ENSO-PDO<br>ENSO-NPI<br>ENSO-NAO<br>PDO-NAO<br>PDO-NPI<br>NAO-NPI | PDO-**NAO**<br>PDO-NPI<br>**NAO**-NPI | YES |
| 8 | GFDL CM2.1 Control run Years 179–187 | ENSO-PDO<br>ENSO-NPI<br>PDO-NPI | None of the pairs | NO |
| 9 | GFDL CM2.1 SRESA1B forced run Years 2027–2032 | ENSO-PDO<br>ENSO-NPI<br>PDO-NPI | ENSO-**NAO**<br>PDO-**NAO** | YES |
| 10 | GFDL CM2.1 SRESA1B forced run Years 2065–2072 | ENSO-PDO<br>ENSO-NPI<br>ENSO-NAO<br>PDO-NPI<br>NAO-NPI | PDO-**NAO** | YES |
| 11 | ECHAM5 control run Years 253–257 | ENSO-PDO<br>ENSO-NPI<br>PDO-NPI | ENSO-NPI<br>ENSO-**NAO**<br>ENSO-PDO<br>**NAO**-NPI | YES |
| 12 | ECHAM5 control run Years 275–280 | ENSO-NAO<br>ENSO-NPI<br>PDO-NAO<br>PDO-NPI<br>NAO-NPI | None of the pairs | NO |

[a]Bold indicates mode that appears to be behind all climate shifts.
[b]NAO coupling with PDO increases after 1936, well after the modes enter the synchronization state.

of 11 years). The correlation relates through formula (1) in auxiliary material to the measure of synchronization. We see that the absolute value of the correlation between pair of modes begins to increase and remains (on the average) at a level of at least 0.5 in that period for all pairs but the ENSO-NPI pair. The value of 0.5 corresponds to the significance level indicated by the horizontal dotted line in Figure 1. Thus, during this event most pairs contribute to synchroni-

zation. This leads to an overall decrease in the distance of the network. Figure 3 offers more insights. Here the broken line is again the distance of the complete network of the four modes and the solid line indicates the coupling between two modes as a function of time with decreasing values corresponding to increasing coupling strength. We observe that when the network enters synchronization at about 1932 the coupling strength decreases for almost all pairs. This leads to the overall coupling strength decrease shown in Figure 1 at the start of the period. This tendency begins to reverse in the late 1930s but this tendency is pronounced only in pairs involving the NAO (Figure 3, right). It thus appears that the mode significantly affecting the overall coupling strength in this case is NAO.

[5] We have repeated the analysis in Figures 2 and 3 for all 12 synchronization events in model simulations and observations (see auxiliary material). Table 1 summarizes the findings. In general Table 1 indicates, as expected, that a pair may be synchronized but not necessarily strongly coupled. The most important finding, however, is that one mode appears to be behind all climate shifts. This mode (highlighted in bold) is the NAO. This north Atlantic mode is without exception the common ingredient in all shifts and when it is not coupled with any of the Pacific modes no shift ensues. In addition, in all cases where a shift occurs NAO is necessarily coupled to north Pacific. In some cases it any also be coupled to the tropical Pacific (ENSO) as well, but in none of the cases NAO is only coupled to ENSO. Thus our results indicate that not only NAO is the instigator of climate shifts but that the likely evolution of a shifts has a path where the north Atlantic couples to north Pacific, which in turn couples to the tropics.

[6] Solid dynamical arguments and past work offer a concrete picture of how the physics may play out. NAO with its huge mass re-arrangement in north Atlantic affects the strength of the westerly flow across mid-latitudes. At the same time through its ''twin'', the arctic Oscillation (AO), it impacts sea level pressure patterns in the northern Pacific. This process is part of the so-called intrinsic mid-latitude northern hemisphere variability [*Vimont et al.*, 2001, 2003]. Then this intrinsic variability through the seasonal ''footprinting'' mechanism [*Vimont et al.*, 2001, 2003] couples with equatorial wind stress anomalies, thereby acting as a stochastic forcing of ENSO. This view is also consistent with a recent studies showing that PDO modulates ENSO [*Gershunov and Barnett*, 1998; *Verdon and Franks*, 2006]. Another possibility of how NAO couples to north Pacific may be through the five lobe circumglobal waveguide pattern [*Branstator*, 2002]. It has been shown that this waveguide pattern projects onto NAO indices and its features contribute to variability at locations throughout northern hemisphere. Finally, north Atlantic variations have been linked to northern hemisphere mean surface temperature multidecadal variability through redistribution of heat within the northern Atlantic with the other oceans left free to adjust to these Atlantic variations [*Zhang et al.*, 2007]. Thus, NAO, being the major mode of variability in the northern Atlantic, impacts both ENSO variability and global temperature variability. Recently a study has shown how ENSO with its effects on PNA can through vertical propagation of Rossby waves influence the lower stratosphere and how in turn the stratosphere can influence NAO through downward progression of Rossby waves [*Ineson and Scaife*, 2009]. These results coupled with our results suggest the following 3-D super-loop NAO → PDO → ENSO → PNA → stratosphere → NAO, which may capture the essence of low-frequency variability in the northern hemisphere.

## 3. Conclusions

[7] Many studies have in the past dealt with the origin and mechanisms of climate oscillations as well as with the consequences of their interactions. Our study with the help of a novel approach identifies for the first time which may be the most significant of these oscillations. In a dynamical scenario where the major modes of variability in the northern hemisphere are synchronized, an increase in the coupling strength destroys the synchronous state and causes climate to shift to a new state. Here we were able to identify that the major participant in this coupling strength increase is NAO, which we found to be behind all climate shifts observed in observations as well as in three climate simulations. Understanding variability of our extremely complex climate system is far from complete as new and often contradicting views are proposed. In this realm we hope that our results will provide some direction and focus to this perpetual quest for understanding climate variability.

## References


Barnston, A. G., and R. E. Livezey (1987), Classification, seasonality, and persistence of low-frequency atmospheric circulation patterns, *Mon. Weather Rev.*, *115*, 1083–1126.

Boccaletti, S., J. Kurths, G. Osipov, D. J. Valladares, and C. S. Zhou (2002), The synchronization of chaotic systems, *Phys. Rep.*, *366*, 1–101.

Branstator, G. (2002), Circumglobal teleconnections, the jet stream waveguide, and the North Atlantic Oscillation, *J. Clim.*, *15*, 1893–1910.

Brohan, P., J. J. Kennedy, I. Harris, S. F. B. Tett, and P. D. Jones (2006), Uncertainty estimates in regional and global observed temperature changes: A new data set from 1850, *J. Geophys. Res.*, *111*, D12106, doi:10.1029/2005JD006548.

Enfield, D. B., A. M. Mestas-Nuñez, D. A. Mayer, and L. Cid-Serrano (1999), How ubiquitous is the dipole relationship in tropical Atlantic sea surface temperatures?, *J. Geophys. Res.*, *104*, 7841–7848.

Gershunov, A., and T. P. Barnett (1998), Interdecadal modulation of ENSO teleconnections, *Bull. Am. Meteorol. Soc.*, *79*, 2715–2725.

Hurrell, J. W. (1995), Decadal trends in the North Atlantic Oscillation regional temperature and precipitation, *Science*, *269*, 676–679.

Ineson, S., and A. A. Scaife (2009), The role of the stratosphere in the European climate response to El Niño, *Nat. Geosci.*, *2*, 32–36.

Kerr, R. A. (2000), A North Atlantic climate pacemaker for the centuries, *Science*, *288*, 1984–1986, doi:10.1126/science.288.5473.1984.

Mantua, N. J., S. R. Hare, Y. Zhang, J. M. Wallace, and R. C. Francis (1997), A Pacific interdecadal climate oscillation with impacts on salmon production, *Bull. Am. Meteorol. Soc.*, *78*, 1069–1079.

Pecora, L. M., T. L. Carroll, G. A. Johnson, and D. J. Mar (1997), Fundamentals of synchronization in chaotic systems, concepts, and applications, *Chaos*, *7*, 520–543.

Philander, G. S. (1990), *El Niño, La Niña, and the Southern Oscillation*, Academic, San Diego, Calif.

Smirnov, D. A., and B. P. Bezruchko (2003), Estimation of interaction strength and direction from short and noisy time series, *Phys. Rev. E*, *68*, 046209.

Trenberth, K. E., and J. W. Hurrell (1994), Decadal atmospheric-ocean variations in the Pacific, *Clim. Dyn.*, *9*, 303–319.

Tsonis, A. A., K. Swanson, and S. Kravtsov (2007), A new dynamical mechanism for major climate shifts, *Geophys. Res. Lett.*, *34*, L13705, doi:10.1029/2007GL030288.

Verdon, D. C., and S. W. Franks (2006), Long-term behaviour of ENSO: Interactions with the PDO over the past 400 years inferred from paleoclimate records, *Geophys. Res. Lett.*, *33*, L06712, doi:10.1029/2005GL025052.

Vimont, D. J., D. S. Battisti, and A. C. Hirst (2001), Footprinting: A seasonal connection between the tropics and mid-latitudes, *Geophys. Res. Lett.*, *28*, 3923–3926.

Vimont, D. J., J. M. Wallace, and D. S. Battisti (2003), The seasonal footprinting mechanism in the Pacific: Implications for ENSO, *J. Clim.*, *16*, 2668–2675.

Wallace, J. M., and D. S. Gutzler (1981), Teleconnections in the geopotential height field during the Northern Hemisphere winter, *Mon. Weather Rev.*, *109*, 784–812.

Zhang, R., T. L. Delworth, and I. M. Held (2007), Can the Atlantic Ocean drive the observed multidecadal variability in Northern Hemisphere mean temperature?, *Geophys. Res. Lett.*, *34*, L02709, doi:10.1029/2006GL028683.

K. L. Swanson and A. A. Tsonis, Atmospheric Sciences Group, Department of Mathematical Sciences, University of Wisconsin-Milwaukee, EMS Building, P.O. Box 413, Milwaukee, WI 53201, USA. (aatsonis@uwm.edu)

G. Wang, Institute of Atmospheric Physics, Chinese Academy of Sciences, Beijing 100029, China.